The Canadian Mineralogist
Vol. 38, pp. 751-761 (2000)

TOPOLOGICAL ENUMERATION OF DECORATED $[Cu^{2+}\phi_2]_N$ SHEETS IN HYDROXY-HYDRATED COPPER-OXYSALT MINERALS

FRANK C. HAWTHORNE§ AND MICHAEL SCHINDLER

Department of Geological Sciences, University of Manitoba, Winnipeg, Manitoba R3T 2N2, Canada

ABSTRACT

Many hydroxy-(hydrated) Cu^{2+} oxysalt minerals, particularly Cu^{2+} sulfates, are based on structural units that are variants of the $[M\phi_2]_N$ sheets of edge-sharing octahedra, where *M* is an octahedrally coordinated cation (including vacancies) and ϕ is an anion. Where $\phi = O^{2-}$,OH,Cl,H_2O, the sheet can be considered as a simple sheet; where $\phi = (SO_4)^{2-}$, the sheet may be considered as a decorated sheet. In such structures, $Cu^{2+}\phi_6$ octahedra show strong axial elongation; Cu^{2+}–ϕ(equatorial) bonds have a bond-valence of ~0.42 *vu*, and Cu^{2+}–ϕ(apical) bonds have a bond-valence of ~0.17 *vu*. Local bond-valence requirements dictate that an $(SO_4)^{2-}$ group can only link to a $[Cu^{2+}\phi_2]_N$ sheet if three Cu^{2+}–ϕ(apical) bonds are incident to the linking anion. This constraint provides considerable restrictions on possible structural arrangements with small unit-cells (<10 Cu^{2+} atoms/plane). These may be derived by two-coloring the 6^3 net. There are currently 20 minerals known that correspond to this structural theme, and it is almost certain that many others await discovery.

Keywords: Cu^{2+} oxysalt minerals, structure topology.

SOMMAIRE

Plusieurs minéraux faisant partie du groupe des oxysels hydroxylés (et hydratés) de Cu^{2+}, et en particulier les sulfates de Cu^{2+}, possèdent des structures fondées sur le motif de feuillets $[M\phi_2]_N$ d'octaèdres à arêtes partagées; ici, *M* est un cation en coordinence octaédrique, ou une lacune, et ϕ représente un anion. Où ϕ représente O^{2-},OH,Cl,H_2O, on peut considérer le feuillet sous sa forme la plus simple; dans les cas où ϕ représente $(SO_4)^{2-}$, on peut considérer l'unité structurale comme feuillet décoré. Dans de telles structures, les octaèdres $Cu^{2+}\phi_6$ font preuve d'un allongement axial remarquable. Les liaisons Cu^{2+}–ϕ équatoriales ont une valence de liaison d'environ 0.42 unités de valence, tandis que pour les liaisons Cu^{2+}–ϕ apicales, elle est d'environ 0.17 unités de valence. D'après les exigeances locales des valences de liaison, un groupe $(SO_4)^{2-}$ ne peut être lié à un feuillet $[Cu^{2+}\phi_2]_N$ que si trois liaisons Cu^{2+}–ϕ apicales impliquent à un anion commun. Cette restriction réduit considérablement les possibilités d'agencements dans le cas de petites mailles (<10 atomes de Cu^{2+} dans un plan). On peut dériver ces possibilités en imposant un schéma bicoloré sur un réseau 6^3. Nous connaissons actuellement vingt minéraux qui correspondent à ce thème structural, et il semble assuré que plusieurs autres restent à découvrir.

(Traduit par la Rédaction)

Mots-clés: oxysels de Cu^{2+}, minéraux, topologie de la structure.

INTRODUCTION

A large number of mineral structures are now known, and it is appropriate that considerable effort should now focus on the development of hierarchical schemes of structure organization (*e.g.*, Liebau 1980, 1985, Moore 1970a, b, 1975, 1982, 1984, Hawthorne 1984, 1985a, 1986, 1990, Sabelli & Trosti-Ferroni 1985). There are a variety of approaches to this problem, but most involve coordination polyhedra and the way in which they link together to form either the complete structure or the strongly bonded part of the structure. Hawthorne (1983) proposed that structural hierarchies be based not on particular chemical classes of minerals (*e.g.*, phosphates, silicates, sulfates) but on general stoichiometries that are written in terms of the strongly bonded coordination polyhedra, and has used this approach (Hawthorne 1985a, 1986, 1990, 1992a, b, 1994) to produce a coherent hierarchical scheme for large groups of oxide and oxysalt structures. Although this scheme is reasonable for most oxide and oxysalt minerals, it must be recognized that some long-range aspects of crystal structures are influenced by local anisotropic electronic effects. Of particular note in this

§ *E-mail address*: frank_hawthorne@umanitoba.ca

regard are the Jahn–Teller effect in Cu^{2+} minerals and stereoactive lone-pair behavior of electrons in such species as As^{3+} and Pb^{2+}.

Eby & Hawthorne (1993) have developed a hierarchical structural classification for Cu^{2+}-oxysalt minerals, dividing them into four classes: isolated polyhedra and finite-cluster structures, infinite-chain structures, infinite-sheet structures, and infinite-framework structures. Eby & Hawthorne (1993) emphasized the variety of Cu^{2+}-oxysalt structures with sheet-like structural units. This is particularly the case with hydroxy–hydrated Cu^{2+}-sulfate minerals, many of which are based on substituted and decorated $[^{[6]}Cu^{2+}\phi_2]$ sheets (ϕ: unspecified anion). There are no corresponding Mg- or Fe^{2+}-sulfate minerals with analogous sheet-like structural units. Furthermore, it is apparent that the local structural response to the electronic degeneracy in holosymmetric [6]-coordinated Cu^{2+} has a major effect on the structural arrangements and stable stoichiometries in Cu^{2+}-oxysalt minerals. Here, we examine the interaction between electronically induced local relaxation, local bond-valence requirements, and the requirements of translational symmetry in controlling structural arrangement and stoichiometry in Cu^{2+} oxysalts based on substituted and decorated $[^{[6]}M\phi_2]$ sheets [*M*: small (*i.e.*, 0.535–0.83 Å) divalent and trivalent cations].

Local Effects

There are two local effects that must be considered here: (1) Jahn–Teller distortion associated with relaxation of the degenerate (or near-degenerate) e_g state in holosymmetric (or reasonably regular) octahedrally coordinated Cu^{2+}, and (2) the requirement that the valence-sum rule be satisfied (Brown 1981): the sum of the bond-valence incident at an atom is approximately equal to its atomic valence.

Jahn–Teller distortion

Jahn & Teller (1937) showed that any non-linear polyatomic molecule with an electronic orbital degeneracy is unstable, and will distort spontaneously to lower the energy of one of the initially degenerate orbitals. For Cu^{2+} in holosymmetric octahedral coordination, the e_g orbitals are energetically degenerate, and simple shielding arguments show that shortening or lengthening of two axial bonds relative to the other four equatorial bonds lifts the orbital degeneracy. These qualitative arguments do not indicate whether extension or contraction of the apical bonds is favored energetically. However, *ab initio* MO (molecular orbital) calculations (Burns & Hawthorne 1990, 1991, 1995a, b, 1996) show that extension of the axial bonds (a [4 + 2] distortion) is energetically favored over contraction of the axial bonds (a [2 + 4] distortion). In accord with this result, Eby & Hawthorne (1993) showed that virtually all $Cu^{2+}\phi_6$ octahedra in Cu^{2+} oxysalt minerals have a [4 + 2] (or similar) arrangement; Cu^{2+}–O(equatorial) values cluster closely round 1.97 Å, and Cu^{2+}–O(apical) values peak at 2.45 Å, although the latter show a wide dispersion, from 2.3 to 3.0 Å. Thus in a $[^{[6]}Cu^{2+}\phi_2]$ sheet, elongate octahedra must occur, rather than the fairly regular octahedra that are characteristic of most other small- and medium-sized (0.535–0.83 Å) divalent and trivalent cations (*i.e.*, *M* cations).

Local bond-valence requirements

The valence-sum rule (Brown 1981) states that the sum of the bond valences incident at an atom is approximately equal to the magnitude of its formal valence. Consider a tetrahedrally or triangularly coordinated oxyanion linked to an $[M\phi_2]_N$ sheet. The local bond-valence environment at the linking simple anion is shown in Table 1 for a range of tetrahedrally and triangularly coordinated cations and a range of simple-anion coordination numbers. As an example, consider an $(SO_4)^{2-}$ [T^{6+}] group: S contributes 1.50 *vu* (valence units) to the linking anion, which thus requires an additional 0.50 *vu* to satisfy its own bond-valence requirements. If the linking anion is [2]-coordinated, it needs a single bond of strength 0.50 *vu*; if the linking anion is [3]-coordinated, it needs two bonds of average strength 0.25 *vu*; if the linking anion is [4]-coordinated, it needs an additional three bonds of average strength 0.17 *vu*. Table 1 lists similar information for other types of cations. In order for a linkage to be stable, it must involve a pattern of bond valences similar to one of those listed in Table 1.

As noted above, $Cu^{2+}\phi_6$ octahedra are invariably [4 + 2]-distorted, with mean equatorial and apical bond-lengths of 1.97 and 2.45 Å, respectively; these bond lengths correspond to bond valences of 0.40 and 0.10 *vu*, respectively. In Table 1, the right-hand column shows the possible patterns of Cu^{2+}–ϕ bonds that satisfy the local bond-valence requirements around the linking anion. Of particular interest is the fact that an $(SO_4)^{2-}$ group can link to a simple anion bonded to three Cu^{2+} cations provided that the anion is involved in a

TABLE 1. POSSIBLE BOND-VALENCE CONFIGURATIONS (*vu*) AROUND ANIONS LINKED TO BOTH *T* AND *M* CATIONS IN AN $[M\phi_2]$ SHEET

*T	s(T–O)	Δs	[2]	[3]	[4]	$M = Cu^{2+}$
T^{6+}	1.50	0.50	0.50 × 1	0.25 × 2	0.17 × 3	3*ap*, *ap* + *eq* + □
T^{5+}	1.25	0.75	–	0.38 × 2	0.25 × 3	2*ap* + *eq*, 2*eq* + □
T^{4+}	1.00	1.00	–	0.50 × 2	0.33 × 3	*ap* + 2*eq*
N^{5+}	1.67	0.33	0.33 × 1	0.17 × 2	0.11 × 3	3*ap*, 2*ap* + □
C^{4+}	1.33	0.67	–	0.33 × 2	0.22 × 3	3*ap*, *ap* + *eq* + □
H_2O	1.60	0.40	0.40 × 1	0.20 × 2	0.13 × 3	3*ap*, *eq* + 2□

*T = tetrahedrally or triangularly coordinated cation: s(T–O) = bond valence of T–O bond; Δs = remaining bond-valence requirement of the O anion; [n] = coordination number of O anion; *ap*, *eq* = apical and equatorial Cu^{2+}–O bonds of approximate strength 0.20 and 0.40 *vu*, respectively.

Cu^{2+}–O(apical) bond in all three constituent octahedra (Fig. 1). Note that the same condition holds for an $(H_2O)^0$ group linked to an $[M\phi_2]_N$ sheet. The two hydrogen atoms provide (on average) 0.80×2 *vu* (Hawthorne 1992a), leaving 0.40 *vu* (Table 1) to be contributed by the *M* cations. Three Cu^{2+}–ϕ(apical) bonds can contribute this amount, allowing (H_2O) to link to (*i.e.*, be a constituent anion of) a $[Cu^{2+}\phi_2]_N$ sheet with essentially the same pattern of bond valences as that required for an $(SO_4)^{2-}$ group to decorate the sheet.

Structural Enumeration

Above, we have shown that in order for an $(SO_4)^{2-}$ group to share a vertex with a $[Cu^{2+}\phi_2]$ sheet, the shared vertex must be incident to three Cu^{2+}–ϕ(apical) bonds. All possible structures based on this theme may thus be evaluated by systematically fitting such arrangements of octahedra into a sheet of octahedra of composition $[M\phi_2]$ such that the valence-sum rule is satisfied at every anion. Consider the structural unit in langite (Fig. 2a): it consists of a continuous sheet of edge-sharing octahedra decorated by $(SO_4)^{2-}$ groups. This representation of the sheet in langite may be simplified by omitting the unshared edges of the octahedra and the Cu^{2+} atoms. The shared edges define a 6^3 net to which the $(SO_4)^{2-}$ groups link from the top and the (H_2O) groups link from the bottom (heavy circles in Fig. 2b). Figure 2c shows the corresponding graph of the bonds in the langite sheet: 6-vertices correspond to Cu^{2+} cations and 3-vertices correspond to anions; Cu^{2+}–ϕ(meridional) bonds are shown as broken lines, Cu^{2+}–ϕ(apical) bonds are shown as full lines. As discussed in a previous section, local bond-valence requirements constrain three Cu^{2+}–ϕ(apical) bonds to meet at an anion of an $(SO_4)^{2-}$ or (H_2O) group (Figs. 2b, c). This requirement is clearly represented in graphical form in Figure 2d: black circles [an anion of the $(SO_4)^{2-}$ group] or hollow circles [(H_2O) groups] occur where three ϕ(apical)–Cu^{2+}–ϕ(apical) linkages (shown as heavy full lines) meet. Note that not all ϕ(apical)–Cu^{2+}–ϕ(apical) linkages must participate in this arrangement as anion coordinations involving only one Cu^{2+}–ϕ(apical) bond do not involve oxyanions or (H_2O) groups (Fig. 2d).

The representation of the langite sheet in Figure 2d suggests a method of enumerating the possible bond-topologies in these types of structure: color one diagonal of each octahedron in a 6^3 net such that the colored diagonals are incident to each other only in triplets [which correspond to complex oxyanions or (H_2O) groups linking to the sheet].

All solutions up to $[Cu^{2+}{}_N\phi_{2N}]$, N = 9, are shown in Figure 3; cell dimensions and layer symmetries are listed in Table 2. The smallest possible unit-cell has N

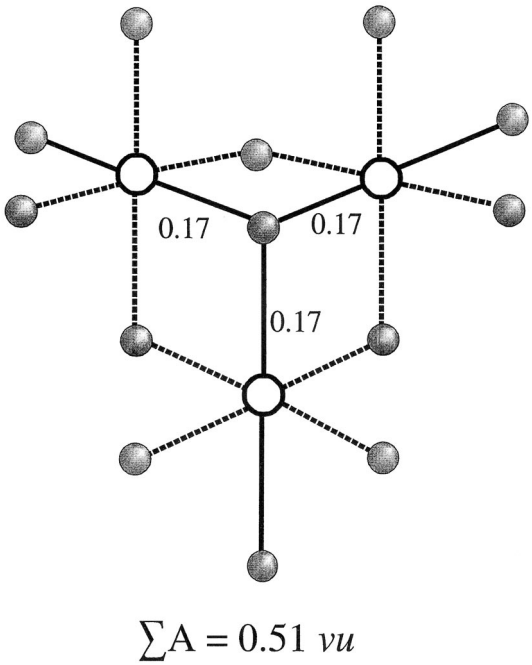

FIG. 1. Ideal bond-valence arrangement for an $(SO_4)^{2-}$ oxyanion to link to a $[Cu^{2+}\phi_2)_N$ sheet; note that three Cu^{2+}–ϕ (apical bonds: solid lines) must be incident at the linking anion (solid circle). The other anions are unshaded circles, the Cu^{2+} cations are small shaded circles, the apical bonds (s = 0.17 *vu*) are solid lines, and the equatorial bonds (s = 0.50 *vu*) are broken lines.

TABLE 2. STRUCTURAL UNIT, CELL DIMENSIONS AND LAYER SYMMETRY OF DECORATED $[M^{2+}\phi_2]_N$ SHEETS WITH $3 \le N \le 9$

Structural unit*	*a* (Å)	*b* (Å)	γ (°)	Layer symmetry	Fig.
$[Cu^{2+}{}_3 X \phi_8]$	5.2	5.2	120	*P*3	3a
$[Cu^{2+}{}_4 X_2 \phi_6]$	6	5.2	90	$P2_1/m$	3b
$[Cu^{2+}{}_4 X_2 \phi_8]$	6	6	120	*P*3	3c
$[Cu^{2+}{}_6 X_2 \phi_{10}]$	9	5.2	90	$P2_1/m$	3d
$[Cu^{2+}{}_6 X_2 \phi_{10}]$	9	5.2	90	$P\bar{1}$	3e
$[Cu^{2+}{}_6 X_2 \phi_{10}]$	8	6	98.3	$P\bar{1}$	3f
$[Cu^{2+}{}_7 X_2 \phi_{12}]$	8	8	120	$P\bar{1}$	3g
$[Cu^{2+}{}_8 X_2 \phi_{14}]$	6	10.4	90	$P\bar{1}$	3h
$[Cu^{2+}{}_8 X_2 \phi_{14}]$	6	10.4	90	$P2_1/m$	3i
$[Cu^{2+}{}_8 X_2 \phi_{14}]$	12	5.2	90	$P\bar{1}$	3j
$[Cu^{2+}{}_6 X_2 \phi_{14}]$	12	5.2	90	$P\bar{1}$	3k
$[Cu^{2+}{}_6 X_2 \phi_{14}]$	12	5.2	90	P1	3l
$[Cu^{2+}{}_8 X_2 \phi_{14}]$	12	5.2	90	$P2_1/m$	3m
$[Cu^{2+}{}_8 X_2 \phi_{14}]$	12	5.2	90	*Pb*	3n
$[Cu^{2+}{}_8 X_2 \phi_{14}]$	12	5.2	90	*P*1	3o
$[Cu^{2+}{}_9 X_3 \phi_{15}]$	9	9	120	*Pm*	3p
$[Cu^{2+}{}_9 X_2 \phi_{16}]$	9	9	120	*Pm*	3q

* $X = (SO_4), (H_2O)$

= 3, with the formula $[Cu^{2+}{}_3\ X\ (OH)_5]$, $X = (SO_4)^{2-}$ or $(H_2O)^o$. A smaller cell is not possible because the requirement that adjacent octahedra be translationally equivalent is not compatible with the requirement that three Cu^{2+}–O(apical) bonds be incident at a single vertex. Inspection of the net in Figure 3a also shows why the sheet must be noncentrosymmetric. Placing a [4 + 2]-distorted octahedron at the origin of the unit cell with the requirement that three Cu^{2+}–ϕ(apical) bonds (shown as heavy lines in Figure 3a) be incident at one of its anions (vertices) forces every other aspect of the unit cell; in particular, if the special anion occurs on the upper level of the sheet of octahedra, then the pseudocentrosymmetrically equivalent anion is forced to participate in one apical and two equatorial Cu^{2+}–ϕ bonds, and hence cannot be an $(SO_4)^{2-}$ or an (H_2O) group. In Figure 3c, some Cu–ϕ(apical) bonds are not involved in linkages to oxyanion or (H_2O) groups; in this arrangement, the direction of the ϕ(apical)–Cu^{2+}–ϕ(apical) bonds is not constrained by the topology of the rest of the structure, and all possible orientations of these bonds are shown by broken lines. For N = 4, there are two possible arrangements (Figs. 3b, c), one of which has an orthogonal cell; both arrangements are forced to be centrosymmetric, and there are no alternative arrangements for each type of cell. There are no possible arrangements for N = 5. For N = 6, there are three arrangements (Figs. 3d–3f) with orthogonal cells; these have tetrahedra on both sides of the sheet. There is only one possibility with N = 7, and this has tetrahedra decorating both sides of the sheet of octahedra (Fig. 3g). There are eight possible arrangements with N = 8 (Figs. 3h–3o), and there are two different orthogonal cells (Table 3); the 6.0 × 10.4 Å cell forces the sheet to be decorated on both sides, whereas the 12.0 × 5.2 Å cell allows decoration on one *or* both sides, a very interesting example of the interaction among bond-valence requirements, electronically driven relaxation and

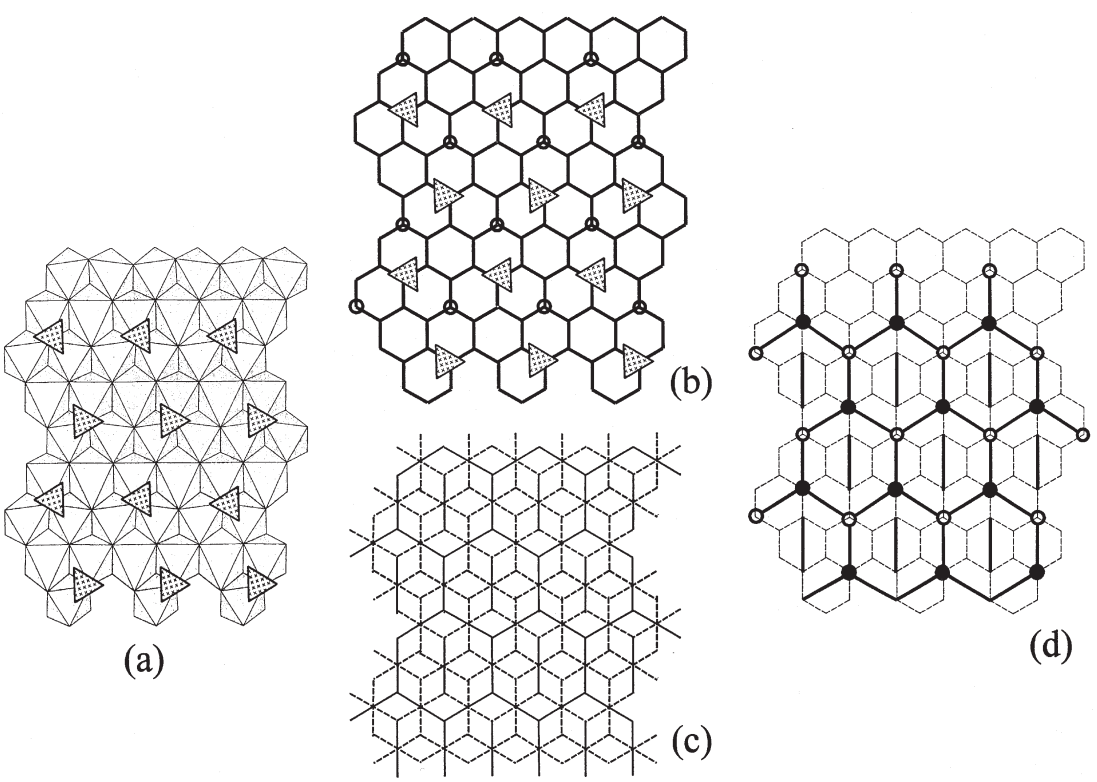

FIG. 2. (a) The decorated $[Cu^{2+}\phi_2]_4$ sheet in langite, $[Cu^{2+}{}_4\ (SO_4)\ (OH)_6\ (H_2O)]\ (H_2O)$, with (SO_4) and (H_2O) groups linked to the $[Cu^{2+}\phi_2]_4$ sheet; (b) the 6^3 net representing the shared octahedron edges of the langite $[Cu^{2+}\phi_2]_4$ sheet embedded into two dimensions. The decorating (SO_4) and (H_2O) (hollow circles) groups link to three-valent vertices above and below the $[Cu^{2+}\phi_2]_4$ sheet, respectively; (c) the 3.6.3.6 net representing the bonds in the $[Cu^{2+}\phi_2]_4$ sheet of langite embedded into two dimensions; 3-vertices represent anions (ϕ) and 6-vertices represent cations (Cu^{2+}); (d) the graph representing the decorated $[Cu^{2+}\phi_2]_4$ sheet of langite; heavy lines are Cu^{2+}–ϕ(apical) bonds, broken lines are shared octahedron edges, solid circles and hollow circles are $(SO_4)^{2-}$ and (H_2O) groups above and below the level of the Cu^{2+} cations, respectively.

TABLE 3. MINERALS BASED ON DECORATED $[M^{2+}\phi_2]_N$ SHEETS, (M = Cu^{2+},Zn)

Mineral	Formula	*a* (Å)	*b* (Å)	*c* (Å)	β (°)	Space gr.	Ref.	Type
Gerhardtite	$[Cu^{2+}_2 (NO_3) (OH)_3]$ (×2)	6.087(4)	5.605(4)	5.597(2)	94.5(1)	$P2_1/m$	[1]	3b
Wroewolfeite	$[Cu^{2+}_4 (SO_4) (OH)_6 (H_2O)] (H_2O)$	6.045(1)	5.646(1)	14.337(2)	93.39(1)	Pc	[2]	3b
Ktenasite	$Zn [(Cu^{2+},Zn)_4 (SO_4)_2 (OH)_6] (H_2O)_6$	5.589(1)	6.166(1)	23.741(7)	95.55(1)	$P2_1c$	[3]	3b
Christelite	$Zn [Cu^{2+}_2 Zn_2 (SO_4)_2 (OH)_6] (H_2O)_4$	5.4143(8)	6.336(1)	10.470(3)	90.06(2)	$P\bar{1}$	[4]	3b
Campigliaite	$Mn [Cu^{2+}_4 (SO_4)_2 (OH)_6] (H_2O)_4$	11.233(7)	6.118(6)	21.725(8)	100.40(5)	$A2$ *	[5]	3b
Niedermayrite	$Cd [Cu^{2+}_4 (SO_4)_2 (OH)_6] (H_2O)_4$	5.535(2)	6.079(1)	21.947(9)	92.04(3)	$P2_1/m$	[6]	3b
Botallackite	$[Cu^{2+}_2 (OH)_3 Cl]$	5.636(1)	6.126(1)	5.717(1)	93.01(1)	$P2_1/m$	[7]	3b
–	$[Cu^{2+}_{2.5} (SO_4) (OH)_3] (H_2O)_3$	6.064(2)	5.496(2)	11.012(6)	92.43(3)	$P\bar{1}$	[8]	3b
Posnjakite	$[Cu^{2+}_4 (SO_4) (OH)_6 (H_2O)]$	10.578(5)	6.345(3)	7.863(3)	117.98(5)	Pa	[9]	3c
Langite	$[Cu^{2+}_4 (SO_4) (OH)_6 (H_2O)] (H_2O)$	7.137(3)	6.031(5)	11.217(1)	90.00(1)	Pc	[10]	3c
Claringbullite	$[Cu^{2+}_4 Cl (OH)_6 (Cl_{0.29}(OH)_{0.71})]$	6.6733(5)	6.6733(5)	9.185(1)	–	$P6_3/mmc$	[11]	3c
–	$[Cd Cu^{2+}_3 (OH)_6 (NO_3)_2] (H_2O)$	6.522(5)	6.522(5)	7.012(6)	–	$P3m1$	[12]	3c
Serpierite	$Ca [Cu^{2+}_4 (SO_4)_2 (OH)_6] (H_2O)_3$	6.250(2)	21.853(2)	22.186(2)	113.36(1)	$B2/b$ *	[13]	4a
Devilline	$Ca [Cu^{2+}_4 (SO_4)_2 (OH)_6] (H_2O)_3$	6.135(2)	22.191(3)	20.870(2)	102.73(2)	$P2_1/b$ *	[14]	4a
Spangolite	$[Cu^{2+}_6 Al (SO_4) (OH)_{12} Cl] (H_2O)_3$	8.254(4)	8.254(4)	14.354(8)	–	$P31c$	[15]	4b
Sabelliite	$[Cu^{2+},Zn)_2 Zn (As,Sb) O_4 (OH)_3]$	8.197(2)	8.197(2)	7.212(1)	–	$P\bar{3}$	[16]	4b
Bechererite	$[Zn_7 Cu^{2+} SiO(OH)_3 (SO_4) (OH)_{13}]$	8.319(2)	8.319(2)	7.377(1)	–	$P\bar{3}$	[17]	4b
Gordaite	$Na [Zn_4 (SO_4) (OH)_6 Cl] (H_2O)_6$	8.3556(3)	8.3556(3)	13.025(1)	–	$P\bar{3}$	[18]	4b
Namuwite	$(Zn,Cu^{2+})_4 (SO_4) (OH)_6 (H_2O)_4$	8.331(6)	8.331(6)	10.54(1)	–	$P\bar{3}$	[19]	4b
–	$Ca [Zn_8 (SO_4)_2 (OH)_{12} Cl_2] (H_2O)_9$	8.3797(4)	8.3797(4)	68.123(5)	–	$R\bar{3}c$	[20]	4b
–	$[Zn_4 (SO_4) (OH)_6] (H_2O)_3$	8.367(3)	8.393(3)	18.569(5)	89.71(3)	$I\bar{1}$	[21]	4b
–	$[Zn_4 (SO_4) (OH)_6] (H_2O)_5$	8.354(2)	8.350(2)	11.001(2)	82.95(2)	$P\bar{1}$	[21]	4b
Chalcophyllite	$[Cu^{2+}_9 Al (AsO_4)_2 (H_2O)_6 (OH)_{12}]_2 (SO_4)_3 (H_2O)_{24}$	10.756(2)	10.754(2)	28.678(4)	–	$R\bar{3}$	[22]	4c
Ramsbeckite	$[(Cu^{2+},Zn)_{15} (SO_4)_4 (OH)_{22}] (H_2O)_6$	16.088(4)	15.576(4)	7.102(2)	90.22(2)	$P2_1/a$	[23]	4d
Schulenbergite	$(Cu^{2+},Zn)_7 (SO_4,CO_3)_2 (OH)_{10} (H_2O)_3$	8.249(1)	8.249(1)	7.183(1)	–	$P\bar{3}$	[24]	–

Synthetic $[Cu^{2+}_{2.5}(SO_4)(OH)_3](H_2O)_3$: α= 102.68(4); γ = 92.06(3)°;
References: (1) Effenberger (1983); (2) Hawthorne & Groat (1985); (3) Mellini & Merlino (1978); (4) Adiwidjaja *et al.* (1996); (5) Sabelli (1982); (6) Giester *et al.* (1998); (7) Hawthorne (1985b); (8) Strandberg *et al.* (1995); (9) Mellini & Merlino (1979); (10) Gentsch & Weber (1984); (11) Burns et al. (1995); (12) Oswald (1969); (13) Sabelli & Zanazzi (1968); (14) Sabelli & Zanazzi (1972); (15) Hawthorne *et al.* (1993); (16) Olmi *et al.* (1995); (17) Hoffmann *et al.* (1997); (18) Adiwidjaja *et al.* (1997); (19) Groat (1996); (20) Burns *et al.* (1998); (21) Bear *et al.* (1986); (22) Sabelli (1980); (23) Effenberger (1988); (24) von Hodenberg *et al.* (1984).

* these structures have been re-oriented such that the $[M\phi_2]$ sheet is parallel to (001).

the requirements of translational symmetry, For N = 9, only two arrangements are possible (Figs. 3p, 3q), and both decorate the sheet of octahedra on both sides.

Occurrence of $[Cu^{2+}\phi_2]_N$ Sheets in Mineral and Inorganic Structures for $3 \le N \le 9$

Table 3 shows mineral and inorganic compounds based on a structural unit consisting of a decorated $[Cu^{2+}\phi_2]_N$ sheet, together with their chemical compositions, space-group symmetries, lattice constants and corresponding graphs. Of course, the unit-cell dimensions and space-group symmetry do not necessarily directly reflect the type of sheet present, as the symmetry of the complete structure is also influenced by the interstitial species, the character of the decorating group, and the geometry of the interactions between the interstitial species and the structural unit. In most cases, the decorating group X is (SO_4), (NO_3), (H_2O) or Cl. Examination of the minerals and inorganic structures containing decorated $[Cu^{2+}\phi_2]_N$ sheets shows that only sheets homeomorphic to graphs 3b and 3c have been discovered so far.

Graph 3b

The sheet of composition $[M_4X_2\phi_6]$ and a = 6.0, b = 5.2 Å, γ = 90° is homeomorphic to graph 3b and has layer symmetry $P2_1/m$. The sheet occurs in botallackite, niedermayrite, campigliaite, ktenasite, wroewolfeite, gerhardtite and christelite, and in the synthetic compound $Cu^{2+}_{2.5} (OH)_3 (SO_4) (H_2O)_2$ (Table 3).

The structures of botallackite, $Cu^{2+}_2 (OH)_3 Cl$, and gerhardtite, $Cu^{2+}_2 (NO_3) (OH)_3$, have space-group symmetry $P2_1/m$. In botallackite, the decorating Cl anion receives 0.55 *vu* from hydrogen bonding and requires an additional 0.183 *vu* from each apical Cu^{2+}–O bond. In gerhardtite, the linking O-atom between the decorating (NO_3) group and the $[Cu^{2+}\phi_2]_4$ sheet receives 1.67 *vu* from N^{5+} and requires an additional 0.11 *vu* from each apical Cu^{2+}–φ bond.

Subgroups of layer symmetry $P2_1/m$ occur in all mineral and inorganic structures in which (SO_4) groups are (part of) the decorating groups (Table 3), *e.g.*, wroewolfeite, in which (H_2O) and (SO_4) groups decorate the $[Cu^{2+}\phi_2]_4$ sheets.

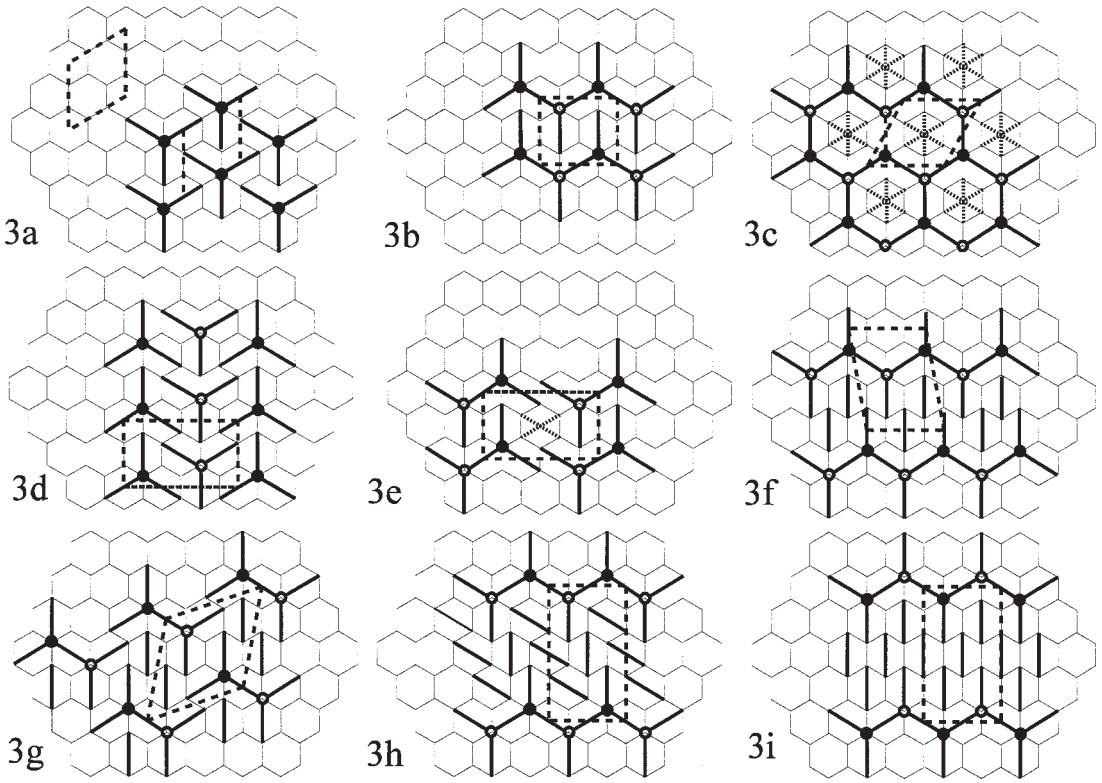

FIG. 3. Graphs of all possible linkages of the decorating $(SO_4)^{2-}$ (H_2O) [+ $(NO_3)^-$ and Cl^-] groups to a $[Cu^{2+}\phi_2]_N$ sheet for $3 \leq N \leq 9$, labeled (3a)–(3q) for convenience of reference; heavy lines are Cu^{2+}–ϕ (apical) bonds, short-dash broken lines are apical bonds which can occur in different orientations, thin lines are shared octahedron edges, solid circles and hollow circles are anions belonging to the decorating groups above and below the level of the Cu^{2+} cations, respectively; long-dash broken lines indicate the two-dimensional unit-cell. Cell dimensions, layer symmetries and formulae are given in Table 2.

Graph 3c

The sheet that is homeomorphic to graph 3c has the composition $[Cu^{2+}_4\ X_2\ \phi_6]$, and the highest possible layer-symmetry of this sheet is $P\bar{3}2/m1$ with $a = b = 6.0$ Å and $\gamma = 120°$. The occurrence of this layer-symmetry depends on the type of the central $(M\phi_6)$ octahedron inside the six-membered ring formed by apical Cu^{2+}–ϕ bonds (Fig. 3c): it occurs if and only if (1) the central octahedron contains six equivalent M–ϕ bonds (the heavy broken lines in Fig. 3c), or (2) there is only short-range order of apical and equatorial bond-orientations such that the long-range symmetry corresponds to (1), or (3) the central M-site is vacant. All subgroups of layer symmetry $P\bar{3}2/m1$ are possible, depending on the orientation of the apical bonds in a central $(Cu^{2+}\phi_6)$ octahedron. Homeomorphisms (see Schindler *et al.* 2000) to graph 3c occur in the sheets of claringbullite, posnjakite and langite, and in the synthetic compound $[Cd\ Cu^{2+}_3\ (OH)_6\ (NO_3)_2\ (H_2O)]$ (Table 3).

In claringbullite, $[Cu^{2+}_4\ Cl\ (Cl_{0.29}\ (OH)_{0.71}\ (OH)_6]$, the M site of the central octahedron is vacant, and the sheet has layer symmetry $P\bar{3}2/m1$. The $(Cu^{2+}\phi_2)_4$ sheet is embedded into a three-dimensional framework that has space-group symmetry $P6_3/mmc$, a supergroup of $P\bar{3}2/m1$ with $t = [2]$ (t = *translationengleich*). The decorating Cl anion is coordinated by two triplets of Cu^{2+} atoms from two adjacent sheets, and receives 0.17 *vu* from each apical bond. The same layer-symmetry occurs in synthetic $[Cd\ Cu^{2+}_3\ (OH)_6\ (NO_3)_2\ (H_2O)]$, in which the central octahedrally coordinated position is occupied by a regular $(Cd\phi_6)$ octahedron with six equivalent Cd–ϕ bonds. The O-atom of the decorating (NO_3) group receives 0.11 *vu* from three apical Cu^{2+}–ϕ bonds. Thus the space-group symmetries of claringbullite and synthetic $[Cd\ Cu^{2+}_3\ (OH)_6\ (NO_2)_2\ (H_2O)]$ are subgroups of layer symmetry $P\bar{3}2/m1$ (Table 3, Fig. 2). In posnjakite, $[Cu^{2+}_4\ (SO_4)\ (OH)_6\ (H_2O)]$, and langite, $[Cu^{2+}_4\ (SO_4)\ (OH)_6\ (H_2O)]\ (H_2O)]$, the central octahedron position is a [4 + 2]-distorted $(Cu^{2+}\phi_6)$ octahedron.

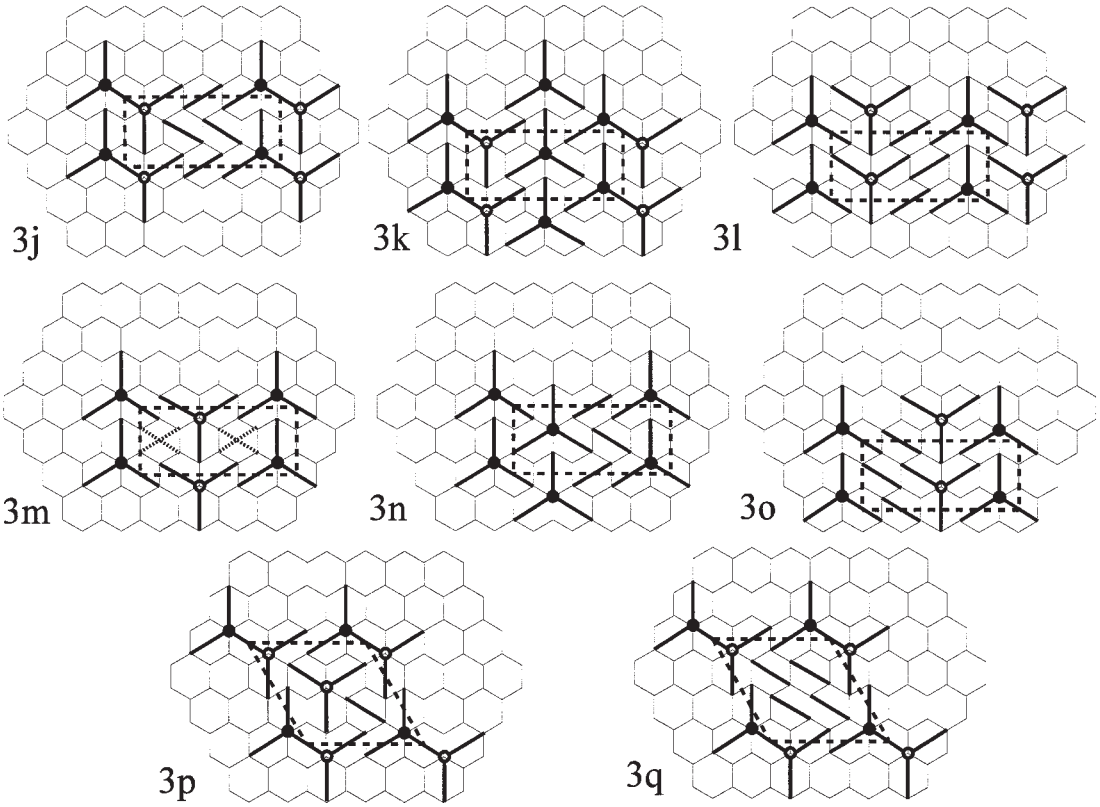

$[Cu^{2+}\phi_2]_N$ Sheets in Minerals and Inorganic Compounds for N > 9

A $[Cu^{2+}\phi_2]_N$ sheet with N = 16 occurs in serpierite and devilline (Table 3). The homeomorphic graph is labeled as 4a in Figure 4. The $[Cu^{2+}\phi_2]_N$ sheet has composition $[Cu^{2+}{}_{16}\, X_8\, \phi_{24}]$ with a = 6.0, b = 20.8 Å and γ = 90°. Here, the highest possible layer-symmetry *is Cm*. The occurrence of this symmetry depends on the type and orientation of the central octahedron (marked with broken lines), *i.e.*, it occurs if the apical bonds of the octahedron are parallel to *b*. This is the case in devilline, $Ca\,[Cu^{2+}{}_4\,(SO_4)_2\,(OH)_6$, in which the glide planes parallel to *b* are retained in the overall space-group: $P2_1/b$. The sheets in serpierite, $Ca\,(Cu^{2+},Zn)_4\,(SO_4)_2\,(OH)_6](H_2O)_3$, also have layer symmetry *Cm* because the central octahedron position is occupied by a regular ($Zn\phi_6$) octahedron. Similar to devilline, the *b*-glide plane of the layer in serpierite is retained in the overall space-group: *B*2/*b*.

Interrupted $[Cu^{2+}\phi_2]_N$ Sheets in Minerals and Inorganic Compounds

An interrupted $[Cu^{2+}\phi_2]_N$ sheet is a sheet that contains vacant octahedral positions, *i.e.*, octahedra with six equivalent *M*–ϕ bonds, or vacancies at the octahedrally coordinated sites, generally associated with tetrahedra linking to the anions surrounding the vacant site. Claringbullite, serpierite and synthetic $[Cd\,Cu^{2+}{}_3\,(OH)_6\,(NO_3)_2\,(H_2O)]$ are examples in which the arrangement of [4 + 2]-distorted octahedra in the $[Cu^{2+}\phi_2]_N$ sheets is interrupted by vacancies or regular (*i.e.*, non-Jahn–Teller distorted) octahedra. Their corresponding homeomorphic graphs can be derived by enumeration because the interruptions do not change the connectivity of the graphs. This is not the case in graphs 4b, 4c and 4d, which occur only if one or more octahedron positions are vacant or occupied by other polyhedra. We have found one type of interrupted sheet in minerals with three-valent black vertices (graph 4b), and we describe two examples of graphs with two-valent or two- and three-valent black vertices (graphs 4c and 4d in Fig. 4).

Graph 4b

The sheet that is homeomorphic to graph 4b has highest possible layer-symmetry $P\bar{3}$ with $a = b$ = 8.0 Å and γ = 120°. Its composition is $[Cu^{2+}{}_7\, X_2\, \phi_{12}]$, and it has the same composition as the sheet that is homeomorphic to graph 3g. Graph 4b was not derived by the topological enumeration described above as its connec-

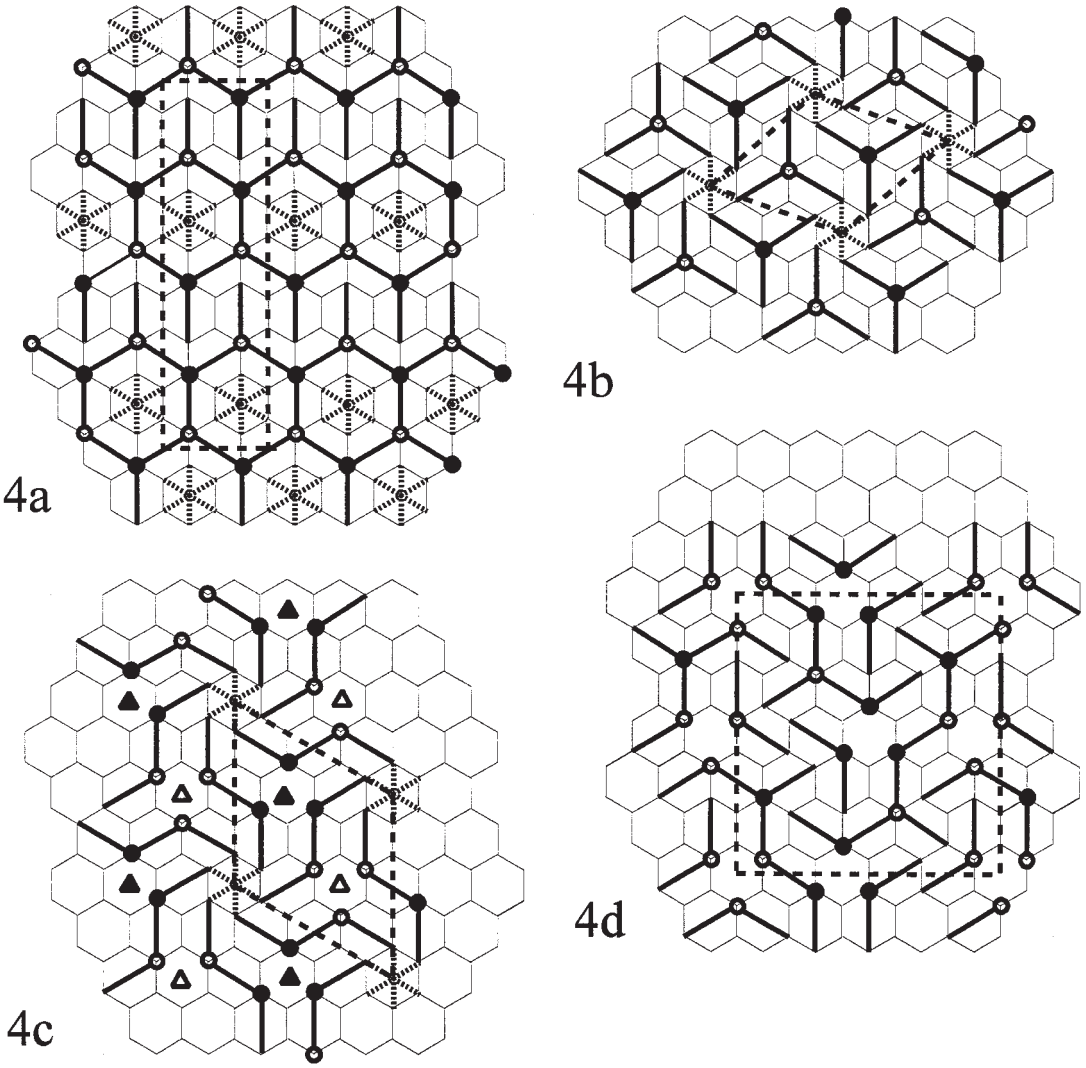

FIG. 4. (a) Graph 4a, which is homeomorphic to a $[Cu^{2+}\phi_2]_N$ sheet with N = 16; the broken lines in the six-membered rings can represent a vacant octahedron position, an octahedron with six equivalent bonds, or different orientations of the apical Cu^{2+}–ϕ bonds; (b) the graph 4b, which is homeomorphic to an interrupted sheet of composition $[Cu^{2+}_7 X_2 \phi_{12}]$; (c) graph 4c, which is homeomorphic to an interrupted sheet with composition $[Cu^{2+}_{12} X_6 \phi_{18}]$; the sheet occurs in chalcophyllite, the six equivalent *M*–ϕ bonds of the ($Al\phi_6$) octahedra are marked with broken lines, and the (AsO_4) tetrahedra are marked by triangles; (d) the graph 4d with two-valent and three-valent black vertices; octahedron positions without solid lines are vacant; all other symbols as in Figure 3.

tivity is only possible where every seventh octahedron position (marked with broken lines in Fig. 4) is vacant or occupied by another kind of polyhedron. Sheets homeomorphic to graph 4b occur in spangolite, sabelliite, gordaite, bechererite and namuwite, and in the synthetic Zn-bearing compounds $[Zn_4 (SO_4) (OH)_6] (H_2O)_3$, $[Zn_4 (SO_4) (OH)_6] (H_2O)_5$ and Ca $[Zn_8 (SO_4)_2 (OH)_{12} Cl_{12}] (H_2O)_9$ (Table 3).

In spangolite, $[Cu^{2+}_6$ Al (SO_4) Cl $(OH)_{12}] (H_2O)_3$, every seventh octahedron position is occupied by a regular ($Al\phi_6$) octahedron; this arrangement retains the layer symmetry $P\bar{3}$ and has seven octahedrally coordinated cations, corresponding to the ideal formula $[Cu^{2+}_7 X_2 \phi_{12}]$. The ($SO_4$) and Cl groups decorate the top and bottom of the $[Cu^{2+}\phi_2]_7$ sheet, respectively. A similar arrangement occurs in sabelliite, $[(Cu^{2+},Zn)_2$ Zn (As,Sb)

$O_4]$ $(OH)_3$, in which every seventh octahedron position is occupied by a regular $(Zn\phi_6)$ octahedron and the decorating groups are $(As\phi_4)$, $(Sb\phi_4)$ and $(Zn\phi_4)$ tetrahedra.

In gordaite, Na $[Zn_4\ (SO_4)\ (OH)_6\ Cl]\ (H_2O)_6$, namuwite, $[(Zn,Cu^{2+})_4\ SO_4\ (OH)_6]\ (H_2O)_4$ and the synthetic inorganic compounds $[Zn_4\ (SO_4)\ (OH)_6]\ (H_2O)_3$, $[Zn_4\ (SO_4)\ (OH)_6]\ (H_2O)_5$ and Ca $[Zn_8\ (SO_4)_2\ (OH)_{12}\ Cl_2]\ (H_2O)_9$, every seventh octahedron position is replaced by two (ZnO_4) tetrahedra that are attached to the sheet above and below this position. All $[M\phi_2]_7$ sheets in these structures have layer symmetry $P3$ and are decorated by (SO_4) tetrahedra. In gordaite, we can rewrite the formula as follows: Na $[Zn_4\ (SO_4)\ (OH)_6\ Cl]\ (H_2O)_6 \times 2 \rightarrow Na_2\ [Zn_8\ (SO_4)_2\ (OH)_{12}\ Cl_2]\ (H_2O)_6 \rightarrow Na_2\ [(Zn_6\square)\ (Zn[OH]_4)_2\ (SO_4)_2\ (OH)_4\ Cl_2]\ (H_2O)_6$. The octahedrally coordinated cation-sites sum to 7; the SO_4 groups link to two X sites, each $Zn(OH)_4$ group links to three OH groups of the sheet, and with the additional four OH and two Cl anions, correspond to the ϕ_{12} anions of the ideal formula. For namuwite, we can rewrite the formula as follows: $\{(Zn,Cu^{2+})_4\ SO_4\ (OH)_6]\ (H_2O)_4 \times 2 \rightarrow [(Zn,Cu)_8\ (SO_4)_2\ (OH)_{12}]\ (H_2O)_8 \rightarrow [\{(Zn,Cu)_6\square\}\ (Zn\phi_4)_2\ (SO_4)_2\ (OH)_6]\ (H_2O)_4$. Thus the octahedrally coordinated sites sum to 7; the SO_4 groups link to the two X sites, each $Zn(OH)_4$ group links to three OH groups of the sheet, and, with the additional $(OH)_6$ anions, correspond to the ϕ_{12} anions of the ideal formula. For Ca $[Zn_8\ (SO_4)_2\ (OH)_{12}\ Cl_2]\ (H_2O)_9$, we can go through a similar procedure to write the formula as Ca $[(Zn_6\square)\ (Zn(OH)_4)_2\ (SO_4)_2\ (OH)_4\ Cl_2]\ (H_2O)_9$. As before, there are seven octahedrally coordinated cation-sites, and the anions sum to $3 \times 2 + 1 \times 2 + 4 + 2 = 14$, as is required by the ideal formula.

In bechererite, $[Zn_7\ Cu^{2+}\ (OH)_{13}\ [Si\ O\ (OH)_3]\ (SO_4)$, every seventh octahedron position is vacant. We may rewrite the chemical formula so that it accords with the crystal structure: $[(\{Zn,Cu^{2+}\}_6\square)\ (\{Zn,Cu\}_2\ \{OH\}_7)\ (SO_4)\ (SiO\{OH\}_3)\ (OH)_6]$. Here, there are seven octahedrally coordinated cation-sites, a sulfate and a silicate group linking to the two X positions, and twelve OH anions, six that link to the two $(\{Zn,Cu\}\phi_4)$ groups and six indicated directly in the formula written above, which thus corresponds to $[Cu^{2+}_7\ X_2\ \phi_{12}]$. The space-group symmetry of the structure is $P3$, a subgroup of the layer symmetry $P3$ by $t = [2]$ (*t = translationengleich*). This symmetry reduction is caused by the ordered arrangement of decorating (SO_4) and (SiO_4) groups.

Graph 4c

Graph 4c is an example of a graph with two-valent black vertices. The homeomorphic sheet has the composition $[Cu^{2+}_{12}\ X_6\ \phi_{18}]$ and layer symmetry $P3$ with $a = b = 10.4$ Å and $\gamma = 120°$ (Fig. 4). This sheet occurs in chalcophyllite, $[Cu^{2+}_9\ Al\ \square_2\ (AsO_4)_2\ (OH)_{12}\ (H_2O)_6]\ (SO_4)_3\ (H_2O)_{24}$ (Table 3). Here, the twelve octahedron positions are occupied by nine [4 + 2]-distorted $(Cu^{2+}\phi_6)$ octahedra, one $(Al\phi_6)$ octahedron with six equivalent M–ϕ bonds (marked with broken lines in Fig. 4) and two vacancies, $\square$. Each vacancy is associated with an AsO_4 group that links to three anions of the sheet, and hence two AsO_4 groups link to the six X sites of the ideal formula. The two-valent black vertices of the apical Cu^{2+}–ϕ bonds are decorated by (H_2O) groups.

Of course, there are more graphs with two-valent black vertices in framework structures. For example, they occur in the corresponding homeomorphic sheets of pseudomalachite, $[Cu^{2+}_5\ (PO_4)_2\ (OH)_4]$ (Shoemaker *et al*. 1977), hydrozincite, $[Zn_5\ (OH)_6\ (CO_3)_2]$ (Ghose 1964) and sclarite, $[(Zn_{2.4}Mg_{1.2}Mn_{0.4})\ Zn_3\ (CO_3)_2\ (OH)_{10}]$ (Grice & Dunn 1989). Here, (PO_4), (ZnO_4) and (CO_3) groups lie above and below vacancies and share two or three anions with the interrupted $[M\phi_2]$ sheets, respectively.

Graph 4d

Graph 4d is an example of a net with two- and three-valent black vertices. The homeomorphic sheet has the composition $(Cu^{2+}_{26}\ X_{16}\ \phi_{36})$ and layer symmetry $P2_1/a$. The sheet occurs in ramsbeckite, $[(Cu^{2+},Zn)_{15}\ (OH)_{22}\ (SO_4)_4]\ (H_2O)_6$ (Table 3). This is not immediately apparent from inspection of the formula of ramsbeckite. However, inspection of the bond lengths shows that Cu^{2+} and Zn are probably quite well ordered in the structure, and that one of the *Zn* sites is tetrahedrally coordinated; thus $(Cu,Zn)_{15}$ becomes $^{[6]}(Cu_{11}Zn_2)\ ^{[4]}(ZnO[OH]_3)_2$. Moreover, the $Zn\phi_4$ tetrahedron shares a vertex with an SO_4 tetrahedron from an adjacent sheet, and hence the tetrahedron part of the structure should be written as $(S\ ZnO_4\ [OH]_3)_2$. The resulting formula is thus $[(Cu_{11}Zn_2)\ (SO_4)_2\ (S\ ZnO_3\ [OH]_3)_2\ (OH)_{16}]\ (H_2O)_6$. The corresponding composition of the sheet is $[Cu^{2+}_{26}\ X_{16}\ \phi_{36}] \rightarrow [Cu^{2+}_{13}\ X_8\ \phi_{18}]_2$. The octahedrally coordinated cations correspond directly. Graph 4d requires eight X positions where tetrahedra are attached to the sheet. In the above formula, there are four SO_4 groups corresponding to four of the X sites. The $Zn\phi_4$ tetrahedra are each attached to three anions of the sheet; two of these anions correspond to X sites (*i.e.*, they link to three octahedrally coordinated cations), and one corresponds to a normal anion. Thus the two $Zn\phi_4$ tetrahedra contribute the other four X sites and an additional two ϕ sites to the ideal formula of $[Cu^{2+}_{13}\ X_8\ \phi_{18}]_2$.

Conclusion

Topological enumeration of $[Cu^{2+}\phi_2]_N$ sheets for $3 \le N \le 9$ results in 17 distinct colored graphs, some of which occur as homeomorphisms in the structures of copper-oxysalt sheet minerals. Further, the enumeration classifies mineral structures in which decorating (SO_4), (CO_3), (NO_3), (H_2O) and (Cl) groups are linked to three apical bonds of [4 + 2]-distorted octahedra in $[M\phi_2]_N$

sheets, and includes also $[Cu^{2+}\phi_2]_N$ sheets that are interrupted by vacancies or undistorted ($M\phi_6$) octahedra.

Acknowledgements

We thank Sergey Krivovichev and Peter Burns for their comments and Bob Martin for his wise(cracking) editing of this paper. Financial support was provided by a Natural Sciences and Engineering Research Council of Canada Research Grant to FCH.

References

Adiwidjaja, G., Friese, K. Klaska, K.-H. & Schlüter, J. (1996): The crystal structure of christelite $Zn_3Cu_2(SO_4)_2(OH)_6{\bullet}4H_2O$. *Z. Kristallogr.* **211**, 518-521.

_____, _____, _____ & _____ (1997): The crystal structure of gordaite $NaZn_4(SO_4)(OH)_6Cl{\bullet}6H_2O$. *Z. Kristallogr.* **212**, 704-707.

Bear, I.J., Grey, I.E., Madsen, I.C., Newnham, I.E. & Rogers, L.J. (1986): Structures of the basic zinc sulfates $3Zn(OH)_2{\bullet}ZnSO_4{\bullet}mH_2O$, m = 3 and 5. *Acta Crystallogr.* **B42**, 32-39.

Brown, I.D. (1981): The bond-valence method: an empirical approach to chemical structure and bonding. *In* Structure and Bonding in Crystals **2** (M. O'Keeffe & A. Navrotsky, eds.). Academic Press, New York, N.Y. (1-30).

Burns, P.C., Cooper, M.A. & Hawthorne, F.C. (1995): Claringbullite: a Cu^{2+} oxysalt with Cu^{2+} in trigonal-prismatic coordination. *Can. Mineral.* **33**, 633-639.

_____ & Hawthorne, F.C. (1990): *Ab initio* molecular orbital studies of copper–oxygen polyhedra. *Geol. Soc. Am., Abstr. Programs* **22**, A259.

_____ & _____ (1991): *Ab initio* molecular orbital studies of copper oxysalt minerals. *Geol. Assoc. Can. – Mineral. Assoc. Can., Program Abstr.* **16**, A17.

_____ & _____ (1995a): Coordination-geometry structural pathways in Cu^{2+} oxysalt minerals. *Can. Mineral.* **33**, 889-905.

_____ & _____ (1995b): Mixed-ligand $Cu^{2+}\phi_6$ octahedra in minerals: observed stereochemistry and Hartree–Fock calculations. *Can. Mineral.* **33**, 1177-1188.

_____ & _____ (1996): Static and dynamic Jahn–Teller effects in Cu^{2+}-oxysalt minerals. *Can. Mineral.* **34**, 1089-1105.

_____, Roberts, A.C. & Nikischer, A.J. (1998): The crystal structure of $Ca[Zn_8(SO_4)_2(OH)_{12}Cl_2](H_2O)_9$, a new phase from slag dumps at Val Varenna, Italy. *Eur. J. Mineral.* **10**, 923-930.

Eby, R.K. & Hawthorne, F.C. (1993): Structural relations in copper oxysalt minerals. I. Structural hierarchy. *Acta Crystallogr.* **B49**, 28-56.

Effenberger, H. (1983): Verfeinerung der Kristallstruktur des monoklinen Dikupfer(II)-trihydroxi- nitrates $Cu_2(NO_3)(OH)_3$. *Z. Kristallogr.* **165**, 127-135.

_____ (1988): Ramsbeckite, $(Cu,Zn)_{15}(OH)_{22}(SO_4)_3{\bullet}6H_2O$: revision of the chemical formula based on a structure determination. *Neues Jahrb. Mineral., Monatsh.*, 38-48.

Gentsch, M. & Weber, K. (1984): Structure of langite, $Cu_4[(OH)_6(SO_4)]{\bullet}2(H_2O)$. *Acta Crystallogr.* **C40**, 1309-1311.

Ghose, S. (1964): The crystal structure of hydrozincite, $Zn_5(OH)_6(CO_3)_2$. *Acta Crystallogr.* **17**, 1051-1057.

Giester, G., Rieck, B. & Brandstätter, F. (1998): Niedermayrite, $Cu_4Cd(SO_4)_2(OH)_6{\bullet}4H_2O$, a new mineral from the Laurion mining district, Greece. *Mineral. Petrol.* **63**, 19-34.

Grice, J.D. & Dunn, P.J. (1989): Sclarite, a new mineral from Franklin, New Jersey, with essential octahedrally and tetrahedrally coordinated zinc: description and structure refinement. *Am. Mineral.* **74**, 1355-1359.

Groat, L.A. (1996): The crystal structure of namuwite, a mineral with Zn in tetrahedral and octahedral coordination, and its relationship to the synthetic basic zinc sulfates. *Am. Mineral.* **81**, 238-243.

Hawthorne, F.C. (1983): Graphical enumeration of polyhedral clusters. *Acta Crystallogr.* **A39**, 724-736.

_____ (1984): The crystal structure of stenonite and the classification of the aluminofluoride minerals. *Can. Mineral.* **22**, 245-251.

_____ (1985a): Towards a structural classification of minerals: the $^{VI}M^{IV}T_2\phi_n$ minerals. *Am. Mineral.* **70**, 455-473.

_____ (1985b): Refinement of the crystal structure of botallackite. *Mineral. Mag.* **49**, 87-89.

_____ (1986): Structural hierarchy in $^{VI}M_x^{III}T_y\phi_z$ minerals. *Can. Mineral.* **24**, 625-642.

_____ (1990): Structural hierarchy in $^{[6]}M^{[4]}T\phi_n$ minerals. *Z. Kristallogr.* **192**, 1-52.

_____ (1992a): The role of OH and H_2O in oxide and oxysalt minerals. *Z. Kristallogr.* **201**, 183-206.

_____ (1992b): Bond topology, bond-valence and structure stability. *In* The Stability of Minerals (G.D. Price & N.L. Ross, eds.). *Mineral. Soc. London, Spec. Pap.* **3**, 25-87.

_____ (1994): Structural aspects of oxide and oxysalt crystals. *Acta Crystallogr.* **B50**, 481-510.

_____ & Groat, L.A. (1985): The crystal structure of wroewolfeite, a mineral with $[Cu_4(SO_4)(OH)_6(H_2O)]$ sheets. *Am. Mineral.* **70**, 1050-1055.

_____, KIMATA, M. & EBY, R.K. (1993): The crystal structure of spangolite, a complex copper sulfate sheet mineral. *Am. Mineral.* **78**, 649-652.

HOFFMANN, C., ARMBRUSTER, T. & GIESTER, G. (1997): Acentric structure (P3) of bechererite, $Zn_7Cu(OH)_{13}[SiO(OH)_3SO_4]$. *Am. Mineral.* **82**, 1014-1018.

JAHN, H.A. & TELLER, E. (1937): Stability of polyatomic molecules in degenerate electronic states. I. Orbital degeneracy. *Proc. R. Soc., Ser.* **A 161**, 220-236.

LIEBAU, F. (1980): Classification of silicates. *Rev. Mineral.* **5**, 1-24.

_____ (1985): *Structural Chemistry of Silicates: Structure, Bonding and Classification*. Springer-Verlag, Berlin, Germany.

MELLINI, M. & MERLINO, S. (1978): Ktenasite, another mineral with $[(Cu,Zn)_2(OH)_3O]^-$ octahedral sheets. *Z. Kristallogr.* **147**, 129-140.

_____ & _____ (1979): Posnjakite, $[Cu_4(OH)_6(H_2O)O]$ octahedral sheets in its structure. *Z. Kristallogr.* **149**, 249-257.

MOORE, P.B. (1970a): Structural hierarchies among minerals containing octahedrally coordinating oxygen. I. Stereoisomerism among corner-sharing octahedral and tetrahedral chains. *Neues Jahrb. Mineral., Monatsh.*, 163-173.

_____ (1970b): Crystal chemistry of the basic iron phosphates. *Am. Mineral.* **55**, 135-169.

_____ (1975): Laueite, pseudolaueite, stewartite, and metavauxite: a study in combinatorial polymorphism. *Neues Jahrb. Mineral., Abh.* **123**, 148-159.

_____ (1982): Pegmatite minerals of P(V) and B(III). *Mineral. Assoc. Can., Short Course Handbook* **8**, 267-291.

_____ (1984): Crystallochemical aspects of the phosphate minerals. In Phosphate Minerals (J.O. Nriagu & P.B. Moore, eds.). Springer-Verlag, Berlin, Germany (155-170).

OLMI, F., SABELLI, C. & TROSTI-FERRONI, R. (1995): The crystal structure of sabelliite. *Eur. J. Mineral.* **7**, 1331-1337.

OSWALD, H.R. (1969): Kristallstruktur von Cadmium-Kupfer-Hydroxidnitrat, $CdCu_3(OH)_6(NO_3)_2H_2O$. *Helv. Chim. Acta* **52**, 2369-2380.

SABELLI, C. (1980): The crystal structure of chalcophyllite. *Z. Kristallogr.* **151**, 129-140.

_____ (1982): Campigliaite, $Cu_4Mn(SO_4)_2(OH)_6{\bullet}4H_2O$, a new mineral from Campiglia Marittima, Tuscany, Italy. II. Crystal structure. *Am. Mineral.* **67**, 388-393.

_____ & TROSTI-FERRONI, R. (1985): A structural classification of sulfate minerals. *Per. Mineral.* **54**, 1-46.

_____ & ZANAZZI, P.F. (1968): The crystal structure of serpierite. *Acta Crystallogr.* **B24**, 1214-1221.

_____ & _____ (1972): The crystal structure of devillite. *Acta Crystallogr.* **B28**, 1182-1189.

SCHINDLER, M., HAWTHORNE, F.C. & BAUR, W.H. (2000): Metastructures: homeomorphisms between complex inorganic structures and three-dimensional nets. *Acta Crystallogr.* **B55**, 811-829.

SHOEMAKER, G.L., ANDERSON, J.B. & KOSTINER, E. (1977): Refinement of the crystal structure of pseudomalachite. *Am. Mineral.* **62**, 1042-1048.

STRANDBERG, H., LANGER, V. & JOHANSSON, L.G. (1995): Structure of $Cu_{2.5}(OH)_3SO_4{\bullet}2H_2O$, a novel corrosion product of copper. *Acta Chem. Scand.* **49**, 5-10.

VON HODENBERG, R., KRAUSE, W. & TÄUBER, H. (1984): Schulenbergit, $(Cu,Zn)_7(SO_4,CO_3)_2(OH)_{10}{\bullet}3H_2O$, ein neues Mineral. *Neues Jahrb. Mineral., Monatsh.*, 17-24.

Received November 8, 1999, revised manuscript accepted March 11, 2000.